

Potential impact of land use change on future regional climate in the Southeastern U.S.: Reforestation and crop land conversion

M. Trail,¹ A.P. Tsimpidi,¹ P. Liu,¹ K. Tsigaridis,^{2,3} Y. Hu,¹ A. Nenes,^{4,5} B. Stone,⁶ and A.G. Russell¹

Received 11 June 2013; revised 1 October 2013; accepted 3 October 2013; published 28 October 2013.

[1] The impact of future land use and land cover changes (LULCC) on regional and global climate is one of the most challenging aspects of understanding anthropogenic climate change. We study the impacts of LULCC on regional climate in the southeastern U.S. by downscaling the NASA Goddard Institute for Space Studies global climate model E to the regional scale using a spectral nudging technique with the Weather Research and Forecasting Model. Climate-relevant meteorological fields are compared for two southeastern U.S. LULCC scenarios to the current land use/cover for four seasons of the year 2050. In this work it is shown that reforestation of cropland in the southeastern U.S. tends to warm surface air by up to 0.5 K, while replacing forested land with cropland tends to cool the surface air by 0.5 K. Processes leading to this response are investigated and sensitivity analyses conducted. The sensitivity analysis shows that results are most sensitive to changes in albedo and the stomatal resistance. Evaporative cooling of croplands also plays an important role in regional climate. Implications of LULCC on air quality are discussed. Summertime warming associated with reforestation of croplands could increase the production of some secondary pollutants, while a higher boundary layer will decrease pollutant concentrations; wintertime warming may decrease emissions from biomass burning from wood stoves.

Citation: Trail, M., A. P. Tsimpidi, P. Liu, K. Tsigaridis, Y. Hu, A. Nenes, B. Stone, and A. G. Russell (2013), Potential impact of land use change on future regional climate in the Southeastern U.S.: Reforestation and crop land conversion, *J. Geophys. Res. Atmos.*, 118, 11,577–11,588, doi:10.1002/2013JD020356.

1. Introduction

[2] Humans have changed the global environment for centuries, and our impact has intensified over recent decades due to increased population and intensification of industrial activity. A considerable forcing for global change is land use and land cover changes (LULCC). The impact of future

LULCC on atmospheric temperatures and global climate is of growing interest as it can impact human and ecosystem health. Increased importance has been given to the study of LULCC impact on climate at a regional level rather than studying the changes in the global mean radiative forcing because “it is the regional responses, not a global average, that produce drought, floods, and other societally important climate impacts” [Mahmood *et al.*, 2010]. The National Research Council (NRC) recently reported that “Improving societally relevant projections of regional climate impacts will require a better understanding of the magnitudes of regional forcings and the associated climate responses” [NRC, 2005]. The NRC includes LULCC as an area that has an impact on climate which is highly variable by region.

[3] Beginning in the 1700s and continuing through the nineteenth century, the southeastern U.S. underwent intense land use and land cover changes [Chen *et al.*, 2006; Pacala *et al.*, 2001; Prestemon and Abt, 2002; Steyaert and Knox, 2008; Wear and Greis, 2002]. The South experienced forest clearing from the 1700s up to the 1930s, a trend which has been reversed in the past few decades with the growth of the timber industry [Wear and Greis, 2002]. Even though there has been significant reforestation since 1930, the 214 million acres of currently forested land in the South only constitutes 60% of the forested land that existed in 1630

Additional supporting information may be found in the online version of this article.

¹School of Civil and Environmental Engineering, Georgia Institute of Technology, Atlanta, Georgia, USA.

²Center for Climate Systems Research, Columbia University, New York, New York, USA.

³NASA Goddard Inst Space Studies, New York, New York, USA.

⁴School of Earth and Atmospheric Sciences, Georgia Institute of Technology, Atlanta, Georgia, USA.

⁵School of Chemical and Biomolecular Engineering, Georgia Institute of Technology, Atlanta, Georgia, USA.

⁶School of City and Regional Planning, Georgia Institute of Technology, Atlanta, Georgia, USA.

Corresponding author: M. Trail, School of Civil and Environmental Engineering, Georgia Institute of Technology, Atlanta, GA 30332, USA. (mcs2rail@gmail.com)

©2013. American Geophysical Union. All Rights Reserved. 2169-897X/13/10.1002/2013JD020356

[Wear and Greis, 2002]. The Southeast now produces 60% of the nation's timber products [Prestemon and Abt, 2002], and in the past 30 years, pine plantations have rapidly increased (from two million acres in 1953 to more than 30 million acres in 1999) [Conner and Hartsell, 2002.]. These trends are slated to continue given the growing demand to develop forest-to-fuel technologies, as well as to increase wood products-related industries. While changes in mobile source fuels may lead to improvements in global climate (or decreases in the projected warming trend) [Bull, 1996; Leiby and Rubin, 2003], the implications of LULCC with regard to climate change are less understood [Akhtar et al., 2008; IPCC (Intergovernmental Panel on Climate Change), 2007; Song et al., 2008; Skamarock et al., 2005; Stooksbury, 2008].

[4] Climate impacts of global- and regional-scale LULCC have been studied using both observations and models [Beltran-Przekurat et al., 2012; Cai and Kalnay, 2004; Chase et al., 2000; Christy et al., 2006; Davin and de Noblet-Ducoudre, 2010; Fall et al., 2010b; Kalnay and Cai, 2003; Lawrence and Chase, 2010; Nunez et al., 2008; Pielke et al., 2011]. Global LULCC studies have shown that afforestation at high latitudes typically tends to warm the atmosphere while afforestation at equatorial latitudes tends to cool. The effects of afforestation at midlatitudes, however, are highly uncertain. Bala et al. [2007] used the Lawrence Livermore National Laboratory Integrated Climate and Carbon model [Bala et al., 2005; Thompson et al., 2004] to simulate the interactions within the climate system including those from LULCC. They found that while the decrease in carbon uptake due to global deforestation would have a warming effect, the biophysical (albedo) changes would induce cooling that would overwhelm the warming associated with carbon in most areas of the globe, particularly in Northern high latitudes. Fall et al. [2010a] used observation minus reanalysis methods to estimate the impacts of historical land cover changes on temperature trends in North America. Fall et al. determined in their study that historical warming trends can be explained on the basis of LULCC, and that climate models should include LULCC along with the typical greenhouse-gas driven radiative forcings. Arora and Montenegro [2011] also simulate future global warming in their study to investigate the impacts of potential realistic LULCC scenarios, rather than extreme cases such as complete deforestation, on climate, where they conclude that any global cooling associated with realistic afforestation is not large enough to take the place of global greenhouse-gas emissions reductions.

[5] More recent global LULCC studies have analyzed the impacts of biophysical changes that impact radiative processes (albedo) as well as those that impact nonradiative processes, such as partitioning of sensible and latent heat transfer [Davin and de Noblet-Ducoudre, 2010; Lawrence and Chase, 2010]. Davin and de Noblet-Ducoudre [2010] used the Institut Pierre-Simon climate model [Marti et al., 2005] to investigate the climate impacts of individual biophysical parameters associated with LULCC. The study reveals the significance of changes in evaporation and surface roughness as well as albedo on climate. Similarly, Lawrence and Chase [2010] use the Community Climate System Model [Lawrence and Chase, 2007] to show that, in some afforested regions, nonradiative processes like evapotranspiration can have a cooling effect that overwhelms warming associated with decreased albedo. Beltran-Przekurat

et al. [2012] also focused on analyzing the effects of changes in heat flux partitioning, surface roughness, and albedo on temperature but concentrated over a region in South America. They found that changes in regional climate are correlated with changes in diurnal heat flux partitioning.

[6] In this paper, we use the spectral nudging technique for dynamic downscaling of global model results to the regional scale and compare resulting climate relevant meteorological fields of two southeastern U.S. LULCC scenarios and a base case scenario for four seasons of the year 2050. The downscaling technique used is a type 4 as discussed by Castro et al. [2005]. In our previous work [Liu et al., 2012], we examined the performance of two nudging techniques, grid and spectral nudging, by downscaling National Centers for Environmental Prediction/National Center for Atmospheric Research data using the Weather Research and Forecasting (WRF) Model and showed that spectral nudging can outperform grid nudging at the small scale while preserving the large scale features. We also compare future versus present day downscaled meteorological fields in previous work [Trail et al., 2013] using spectral nudging to downscale the NASA Goddard Institute for Space Studies (GISS) global climate model E results during the years 2006 to 2010 and 2048 to 2052 over the continental United States and predicted an average warming of 1–3°C during the summer and fall in the southeastern U.S. In this study, we use the same approach to simulate meteorological fields for the year 2050 for current day LULCC, a reforested Southeast scenario, and an increased cropland scenario. The role of specific processes and parameters are investigated. We also discuss some of the implications of LULCC on regional air quality. The downscaling technique and choice of physics parameterizations used were evaluated in Trail et al. [2013] by comparing them with in situ observations for the present year.

2. Model Approach

2.1. Global Model

[7] Lateral boundary and initial conditions for the regional forecast modeling are taken from the GISS ModelE2 (G. A. Schmidt et al., Configuration and assessment of the GISS ModelE2 contributions to the CMIP5 archive, *Journal of Climate*, manuscript in preparation, 2013). The model has a horizontal resolution of $2^\circ \times 2.5^\circ$ latitude by longitude. The model has 40 layers which follow a sigma coordinate up to 150 hPa, with constant pressure layers between 150 and 0.1 hPa. Simulations are carried out for the calendar years 2006–2010 and 2048–2052 with a 3 year spin-up time for each period, driven by possible future atmospheric conditions over the 21st century and follow the scenario development process for Intergovernmental Panel on Climate Change AR5. This study uses the “Representative Concentration Pathway” (RCP) 4.5 scenario [Lamarque et al., 2011; Moss et al., 2010], where global emissions of greenhouse gases, short-lived species, and land-use-land-cover produce an anthropogenic radiative forcing at 4.5 W m^{-2} (approximately 650 ppm CO_2 -equivalent) in the year 2100 [2010]. Physical and chemical parameters were produced at 6 h intervals for regional downscaling by WRF (section 2.2). Further details of the global simulations can be found in Trail et al. [2013].

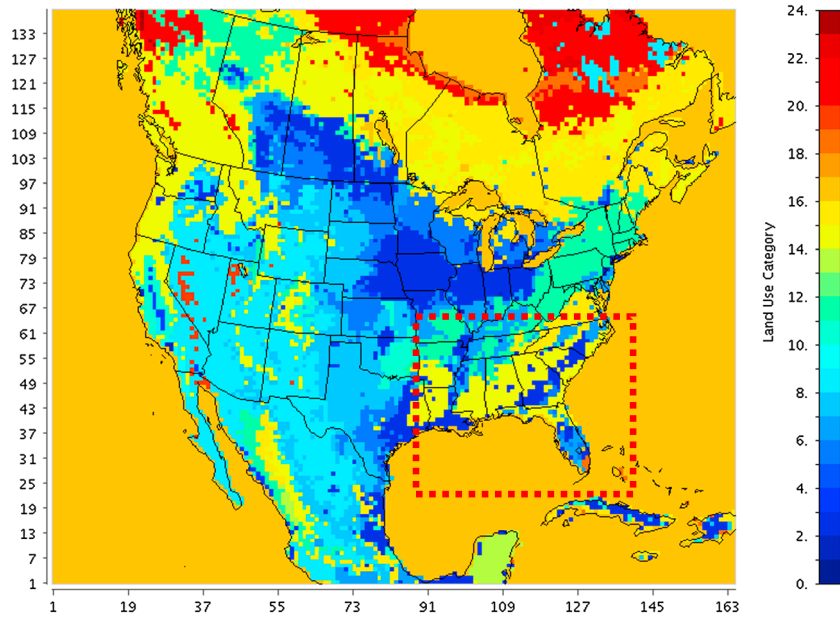


Figure 1. Original dominant land use map of the base case simulation. The area of the tested LULCC scenarios is also shown (red dashed box). Land use category numbers from the legend correspond to categories in Table 1.

2.2. Regional Model

[8] The Weather Research and Forecasting (WRF) Model [Skamarock and Klemp, 2008] version 3.4 is used as the regional simulation model. The modeling domain includes the contiguous United States, southern Canada, and northern Mexico. The domain is centered at 40°N and 97°W with dimensions of 164 × 138 horizontal grids cells (5940 × 5004 km) with 36 km horizontal grid-spacing and the top level at 50 hPa (~15.9 km above ground) (Figure 1). Planetary boundary layer dynamics are simulated using the Yonsei University [Hong et al., 2006] scheme; the Noah scheme [Ek et al., 2003] is used for land surface model. The long-wave Rapid Radiative Transfer Model [Mlawer et al., 1997] and Dudhia scheme [Dudhia, 1989] are used for longwave and shortwave radiation, respectively. A revised version of the Kain-Fritsch scheme [Kain and Fritsch, 1993] is used to represent the effects of both

deep and shallow cumulus clouds, while cloud microphysics are simulated based on Lin et al. [1983].

[9] Key parameters used by WRF associated with LULCC that impact climate include albedo, stomatal resistance (RS), leaf area index (LAI), and surface roughness (Z^0) [Pielke et al., 1998]. Albedo is the fraction of solar energy reflected. Stomatal resistance refers to the leaf’s resistance to release moisture into the atmosphere, affecting whether energy is released as sensible or latent heat. Leaf area index is defined as the one-sided green leaf area per unit ground surface area ($LAI = \text{leaf area}/\text{ground area}, \text{m}^2/\text{m}^2$). The LAI and stomatal resistance are used by the Noah scheme to calculate transpiration via the Jarvis mechanism which also takes into account water availability, photosynthetically active radiation, and CO₂ concentration. Surface roughness is a parameter used to calculate the turbulent diffusion of energy and represents

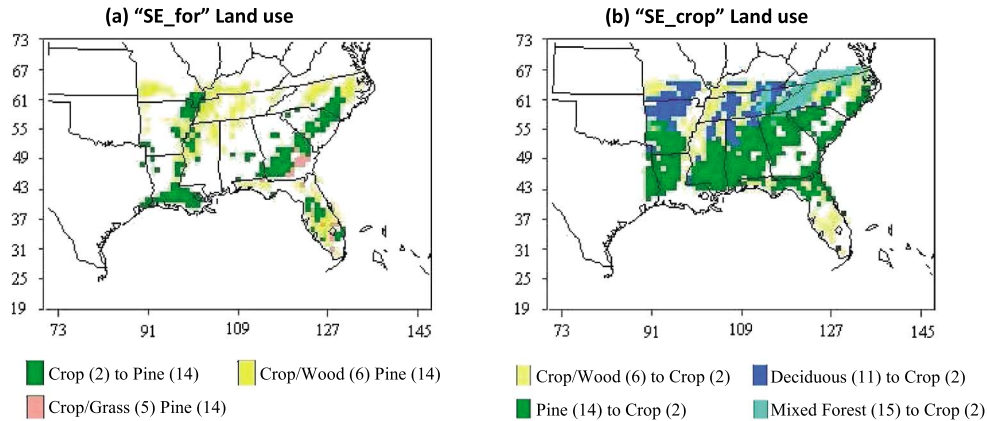


Figure 2. Spatial maps of the dominant land use covers that changed to (a) pine and (b) crop in the SE_for and SE_crop scenario, respectively. Land use category numbers in parentheses correspond to categories in Table 1.

Table 1. USGS Land Use Categories and Relevant WRF Parameters^a

Land Use Category	RS	LAIMIN (area/area)	LAIMAX (area/area)	ALBEDOMIN	ALBEDOMAX	Z0MIN (m)	Z0MAX (m)	
1	“Urban and Built-Up Land”	200	1	1	0.15	0.15	0.5	0.5
2	“Dryland Cropland and Pasture”	40	1.56	5.68	0.17	0.23	0.05	0.15
3	“Irrigated Cropland and Pasture”	40	1.56	5.68	0.2	0.25	0.02	0.1
4	“Mixed Dry/Irr. Cropland and Pasture”	40	1	4.5	0.18	0.23	0.05	0.15
5	“Cropland/Grassland Mosaic”	40	2.29	4.29	0.18	0.23	0.05	0.14
6	“Cropland/Woodland Mosaic”	70	2	4	0.16	0.2	0.2	0.2
7	“Grassland”	40	0.52	2.9	0.19	0.23	0.1	0.12
8	“Shrubland”	300	0.5	3.66	0.25	0.3	0.01	0.05
9	“Mixed Shrubland/Grassland”	170	0.6	2.6	0.22	0.3	0.01	0.06
10	“Savanna”	70	0.5	3.66	0.2	0.2	0.15	0.15
11	“Deciduous Broadleaf Forest”	100	1.85	3.31	0.16	0.17	0.5	0.5
12	“Deciduous Needleleaf Forest”	150	1	5.16	0.14	0.15	0.5	0.5
13	“Evergreen Broadleaf Forest”	150	3.08	6.48	0.12	0.12	0.5	0.5
14	“Evergreen Needleleaf Forest”	125	5	6.4	0.12	0.12	0.5	0.5
15	“Mixed Forest”	125	2.8	5.5	0.17	0.25	0.2	0.5
16	“Water Bodies”	100	0.01	0.01	0.08	0.08	0.0001	0.0001
17	“Herbaceous Wetland”	40	1.5	5.65	0.14	0.14	0.2	0.2
18	“Wooded Wetland”	100	2	5.8	0.14	0.14	0.4	0.4
19	“Barren or Sparsely Vegetated”	999	0.1	0.75	0.38	0.38	0.01	0.01
20	“Herbaceous Tundra”	150	0.41	3.35	0.15	0.2	0.1	0.1
21	“Wooded Tundra”	150	0.41	3.35	0.15	0.2	0.3	0.3
22	“Mixed Tundra”	150	0.41	3.35	0.15	0.2	0.15	0.15
23	“Bare Ground Tundra”	200	0.41	3.35	0.25	0.25	0.05	0.1
24	“Snow or Ice”	999	0.01	0.01	0.55	0.7	0.001	0.001

^aParameters include stomatal resistance (RS), maximum and minimum leaf area index (LAIMAX, LAIMIN), maximum and minimum albedo (ALBEDOMAX, ALBEDOMIN), and maximum and minimum roughness height (Z0MAX, Z0MIN).

the height of the land cover, and affects whether energy is transferred to the atmosphere as sensible or latent heat. Here the MM5 Monin-Obukhov surface layer scheme in WRF uses the surface roughness to calculate latent and sensible heat flux via standard similarity functions.

[10] In the USGS 24-category land use data set, the standard data currently used for WRF simulations, the Southeast is primarily made up of evergreen needleleaf forest, dryland cropland and pasture, deciduous broadleaf forest, and mixtures of these. Two southeastern LULCC scenarios and a base scenario were simulated in this study (Figure 2): one in which all types of current cropland are replaced by evergreen needleleaf (“SE_for”), and one in which all types of forest or forest mixture are replaced by dryland cropland and pasture (“SE_crop”). Evergreen needleleaf forest is chosen due to its commercial use. Evergreen needleleaf forest in the USGS data set

is a combination of the various species of evergreen needleleaf trees and does not differentiate loblolly and slash pine from other species, which may have different physiological characteristics. Loblolly and slash pine make up the majority of the species of pine in the Southeast. Dryland cropland and pasture in the USGS data set includes semi-irrigated crops, or crops that are irrigated with overhead sprinklers, which make up most of the cropland in the Southeast. There is an irrigated cropland category, but this refers to heavily irrigated crops such as rice paddies and is not prevalent in the Southeast where crops are made up of cotton, wheat, corn, and others. The base case simulation will be referred to as SE_norm.

[11] In addition, sensitivity analyses are conducted to determine which model land use parameters have the greatest influence on regional climate and how changes in those parameters affect results. We calculated the sensitivity of

Table 2. Parameterizations Used for Each of the Sensitivity Analyses^a

Sensitivity Case	“Dryland Cropland and Pasture” Parameters						
	RS	LAIMIN (area/area)	LAIMAX (area/area)	ALBEDOMIN	ALBEDOMAX	Z0MIN (m)	Z0MAX (m)
Base	40	1.56	5.68	0.17	0.23	0.05	0.15
ALBp	40	1.56	5.68	0.12	0.12	0.05	0.15
Z ⁰ p	40	1.56	5.68	0.17	0.23	0.5	0.5
RSp	125	1.56	5.68	0.17	0.23	0.05	0.15
LAIp	40	5	6.4	0.17	0.23	0.05	0.15
ALBd	40	1.56	5.68	0.16	0.17	0.05	0.15
Z ⁰ d	40	1.56	5.68	0.17	0.23	0.5	0.5
RSd	100	1.56	5.68	0.17	0.23	0.05	0.15
LAI d	40	1.85	3.31	0.17	0.23	0.05	0.15

^aParameters include minimum stomatal resistance (RS), maximum and minimum leaf area index (LAIMAX, LAIMIN), maximum and minimum albedo (ALBEDOMAX, ALBEDOMIN), and maximum and minimum roughness height (Z0MAX, Z0MIN). The name of each sensitivity case begins with the parameter that changed and ends with “p” or “d” indicating whether the new parameter is from the pine (p) or deciduous (d) land use category. The affected parameters in each case are highlighted in bold.

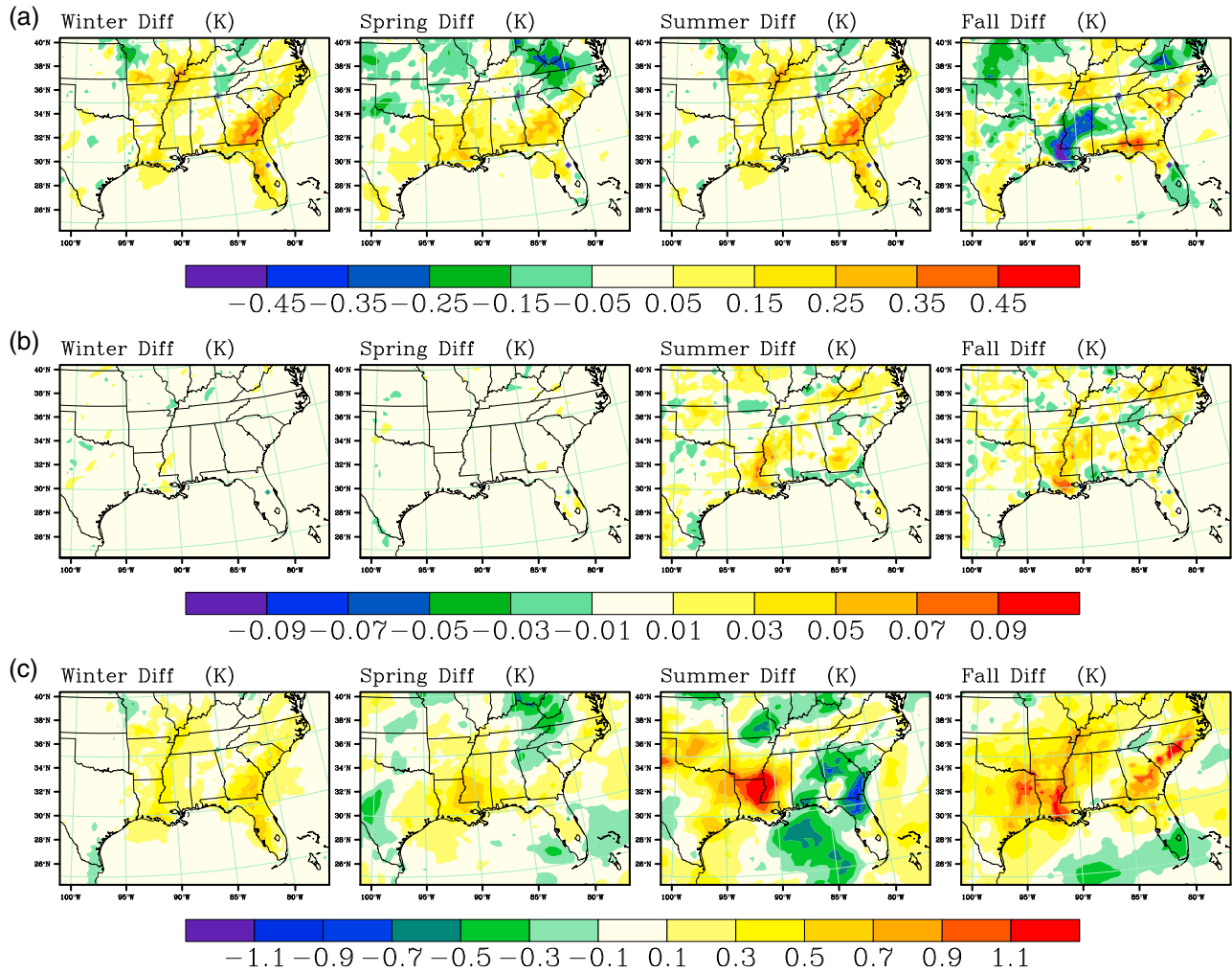


Figure 3. (a) Simulated temperature, (b) soil moisture, and (c) equivalent temperature change of SE_{for} minus SE_{norm} scenario during the four seasons of the year 2050.

regional meteorological variables to individual parameters including surface roughness height (Z^0), albedo, leaf area index (LAI), emissivity, and stomatal resistance (RS). Wintertime (DJF) and summertime (JJA) sensitivities to a parameter are calculated by changing the dryland/cropland parameter of interest to that of evergreen needleleaf land cover and separately to that of deciduous broadleaf forest. Sensitivity simulations are conducted for 3 month periods. Table 1 contains details of the vegetative parameters, and Table 2 contains the sensitivity test parameters. The resulting seasonal mean meteorology is then compared to the base case meteorology over regions where dryland/cropland is the dominant land use.

[12] We do not include simulated changes in atmospheric composition-induced radiative forcing due to LULCC, such as the change in greenhouse gases due to carbon uptake of crops and forests or the changes in the direct and indirect aerosol effect associated with changes in biogenic emissions and air quality.

2.3. Dynamical Downscale of Global Results

[13] Spectral nudging is used with a wave number of 2 in both zonal and meridional directions to account for the large-scale GCM simulation but allow the small scale

features expected from LULCC in the southeastern U.S. to freely develop [Liu *et al.*, 2012]. In other words, no nudging is conducted at wavelengths shorter than the preset value. A wavelength of 2 corresponds to about 1500 km, which is larger than the spatial scale of changes simulated here. Spectral nudging is applied to temperature, horizontal winds, and geopotential height. No nudging is conducted for variables within the planetary boundary layer (PBL), with the exception of the horizontal winds which are nudged at all vertical levels. The nudging coefficient for all nudged variables was set to $3 \times 10^{-4} \text{ s}^{-1}$ [Stauffer and Seaman, 1990]. Nudging is conducted every 6 h during the simulation, consistent with the frequency of the global model data.

[14] Trail *et al.* [2013] found that the model predictions agree well with observations when conducted for 2010. They show that the simulated temperature agrees best with surface observations over the southern U.S., particularly during summer. Simulated wind speed had a root-mean-square error (RMSE) as low as 2.2 m s^{-1} over the South. While details of the base simulation are given in Trail *et al.* [2013], they are briefly summarized here in Tables S1 and S2 in the supporting information.

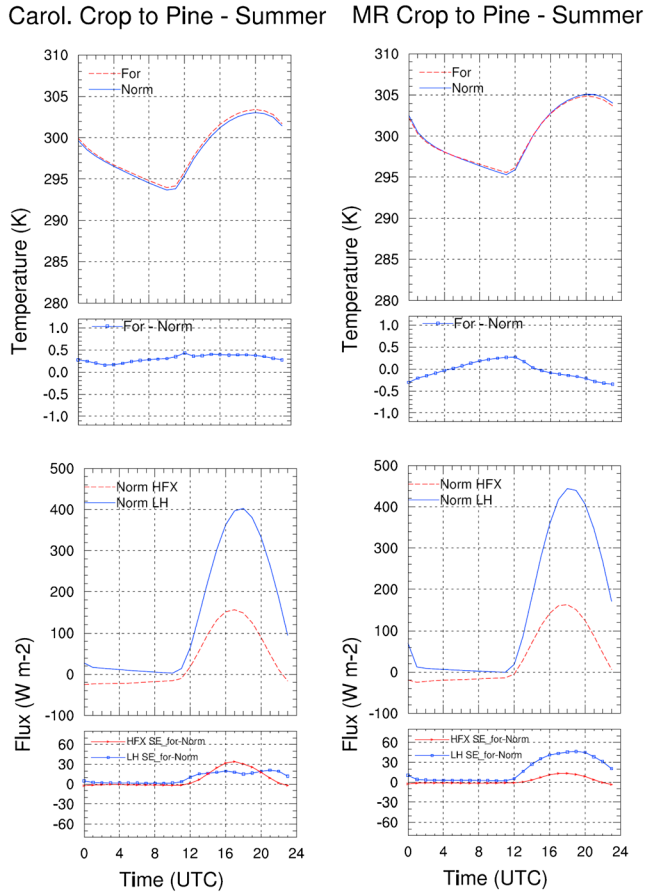


Figure 4. Average diurnal temperature and heat flux trends and anomalies over the grid cells where the dominant land use is converted from crop to pine and separated by the Carolinas and Mississippi river (MR) regions during summer of the year 2050. (top row) Average diurnal temperature by region and season for “SE_norm” and “SE_for”. (second row) Average diurnal temperature anomaly by region and season (“SE_for” minus “SE_norm”). (third row) Average diurnal sensible (red) and latent (blue) heat flux to the atmosphere for the “SE_norm” case. (bottom row) Average diurnal sensible (red) and latent (blue) heat flux anomalies (“SE_for” minus “SE_norm”).

3. Results

3.1. Southeast Reforestation Scenario (“SE_for”)

3.1.1. Land Cover Change and Affected Parameters

[15] The two major LULCC occurring in the Southeast reforestation scenario are the conversion of dryland/cropland and pasture to evergreen needleleaf forest (which will be referred to as “crop” and “pine”, respectively) and conversion of cropland/woodland mosaic (or “crop/wood”) to pine (Figure 2). It is important to note that crop/wood has parameters that represent a combination of not only crop and pine but also of deciduous broadleaf forest. There is also a small region in South Georgia where cropland/grassland mosaic is converted to pine; however, this region is small compared to the other two LULCC. A large region of crop is converted to pine in southern Louisiana and continuing north along the western borders of Mississippi and Tennessee. Crop is also

converted to pine in Florida and in a large region beginning in South Georgia and continuing in a streaking pattern across the eastern regions of South and North Carolina. Crop/wood is converted to pine in the northern regions of the land cover change area including Missouri, Tennessee, and North Carolina, as well as regions in western Mississippi and some in the middle of Florida.

[16] In this simulation the albedo of pine is 0.12 all year, meaning that, within that land use category, 12% of the incoming solar radiation is reflected away from the Earth’s surface (Table 2). The albedo of crop, on the other hand, is higher than pine and changes from 0.17 to 0.23 depending on the time of year, with the lowest albedo occurring when crops are green and the higher when cropland appears whiter and there is increased soil exposure after harvest. Impacts of snow cover on albedo are simulated as well. Correspondingly, in regions where crop is converted to pine, the albedo change causes 10–12% less reflected solar radiation during the winter and fall and only 5–10% less during the spring and summer (Figure S1a, supporting information). The albedo of crop/wood varies from 0.16 to 0.2 depending on the time of year, and the corresponding decreased albedo and seasonal change is reflected in Figure S1a over regions where crop/wood is converted to pine.

[17] The LAI is correlated to albedo since a higher leaf area index usually means more green area to absorb sunlight. However, the combined effect of LAI and stomatal resistance plays another important role in climate, because it drives sensible and latent heat flux partitioning via transpiration. Heat flux partitioning, in turn, strongly impacts temperature and planetary boundary layer (PBL) dynamics [Pielke *et al.*, 1998]. In WRF, the RS is calculated using the Jarvis mechanism where a minimum RS is adjusted by various forcings (i.e., sunlight, temperature, relative humidity, and soil moisture availability). RS for crop and pine are 40 and 125 $s\ m^{-1}$, respectively. In other words, pine trees are more resistant to releasing water and latent heat than crops. During the winter, the LAI increases by up to 4 units (leaf area per area) in regions where the land cover is converted to pine (Figure S1b). Similar to the change in albedo, the difference in LAI decreases during the spring and more so during the summer as crops grow and produce more leaves. During summer, in regions where crop changes to pine, the difference in LAI is only slightly positive (less than 1 unit $area\ area^{-1}$), while the LAI difference is higher (up to 2.5 units $area\ area^{-1}$) in regions where crop/wood changes to pine. We see a greater difference in LAI over regions where crop/wood changes to pine during the summer because, as mentioned earlier, crop/wood includes some parameters from deciduous broadleaf forest which has a lower LAI than that of pine.

[18] Changing surface roughness impacts turbulence within the boundary layer which affects the transfer of momentum, heat, and water vapor from the Earth’s surface. Increasing Z^0 causes more energy to be transferred as latent heat and less as sensible heat. However, the direct implications with regard to climate change are not very well known [Davies and de Noblet-Ducoudre, 2010]. The Z^0 of pine and crop/wood remain constant throughout the year at 0.5 m and 0.2 m, respectively, while the Z^0 of crop (between 0.05 and 0.15 m) is smaller during the winter (Table 1). Again, as crops grow during the spring and summer, the difference in Z^0 decreases slightly in regions where crop is converted to pine.

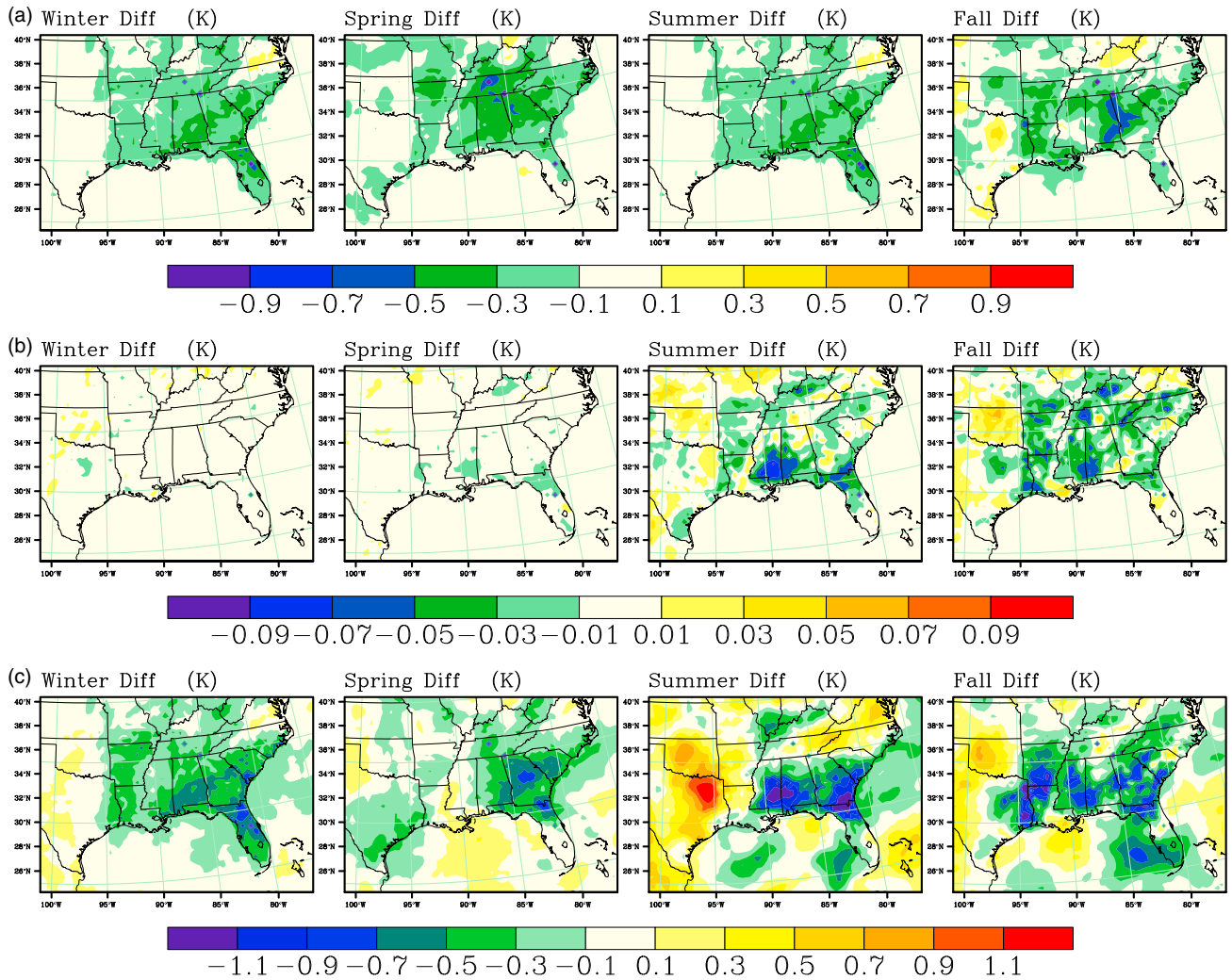


Figure 5. (a) Simulated temperature, (b) soil moisture, and (c) equivalent temperature change of SE_{crop} minus SE_{norm} scenario during the four seasons of the year 2050.

3.1.2. Impacts on Meteorology

[19] A heating pattern of up to 0.5° occurs during the winter over most of the areas where crop and crop/wood are converted to pine (Figure 3a). P values resulting from a paired t test show significant temperature anomalies over regions that are converted to pine (Figure S2). The average diurnal changes in temperature over regions where crop is converted to pine show that this heating occurs during the day, while at night the temperature does not change nearly so much (Figures S3 and S4). The decreased albedo attributed to converting from inactive and exposed soil crop to green pine during the winter drives the heating in these regions (Figure S1a). However, since Z^0 increases with pine reforestation, the winter heating is diminished slightly, although not overcome, by the increase in latent heat flux via evapotranspiration. Also, the daytime boundary layer height increases by 10% on average where crop is converted to pine because more of the energy flux is realized as sensible heat (Figure S3) [Pielke *et al.*, 1998]. During the spring we see a similar heating of around 0.3° mostly over regions where crop is converted to pine. We did not find significant changes in precipitation due to the LULCC perturbations.

[20] Interesting patterns of cooling in Louisiana near the Mississippi river (up to 0.5° decrease) and warming in South Carolina and southern Georgia (up to 0.5° increase) over regions where crop is converted to pine occur during the summer and continue through the fall (Figure 3a). Changes in precipitation may explain some cooling during the summer when Louisiana receives approximately 2 mm more rain per day in the afforested scenario, while net rain near the eastern coast changes little. However, during the fall, there is little apparent change in precipitation over the two regions (Figure S5). Despite little differences in precipitation, there is still an increase in soil moisture in Louisiana during both summer and fall (Figure 3b). Pine has a higher RS and, over time, water is allowed to accumulate throughout the season in the soil near the Mississippi river rather than be evaporated. Correspondingly, the diurnal latent heat flux in Louisiana increases during the daytime in the summer, cooling the surface air, while in Georgia and the Carolinas, the increase in latent heat flux is not as strong, leading to an increase in sensible heat flux to maintain the energy balance, causing the warming (Figure 4). Recent

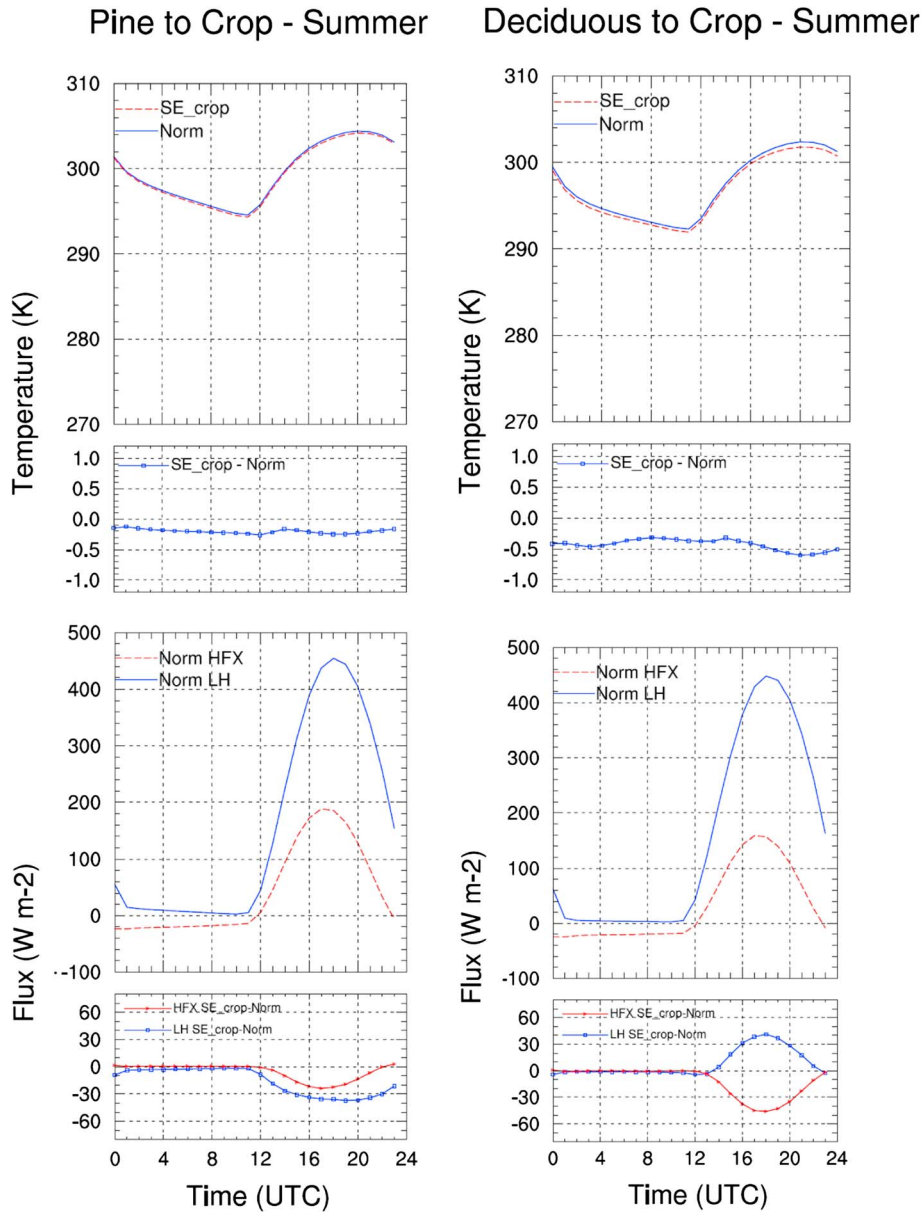


Figure 6. Average diurnal temperature and heat flux trends and anomalies over the grid cells where the dominant land use is converted (left column) from pine to crop and (right column) from deciduous to crop during summer of the year 2050. (top row) Average diurnal temperature by season for “SE_norm” and “SE_crop”. (second row) Average diurnal temperature anomaly by season (“SE_crop” minus “SE_norm”). (third row) Average diurnal sensible (red) and latent (blue) heat flux to the atmosphere for the “SE_norm” case. (bottom row) Average diurnal sensible (red) and latent (blue) heat flux anomalies (“SE_crop” minus “SE_norm”).

studies show that temperature changes alone do not completely characterize changes in surface air heat content because some energy is stored in moisture in the air, and suggest using an equivalent temperature which takes into account the latent heat energy [Fall et al., 2010a]. While cooling occurs during the summer and fall over the Mississippi river, the change in equivalent temperature (Figure 3c) shows an increase in surface heat air content equivalent to up to a degree.

3.2. Southeast Cropification Scenario (“SE_crop”)

3.2.1. Land Cover Change and Affected Parameters

[21] There are four major LULCC that occur in the Southeast cropification scenario where the following four land covers are converted to dryland/cropland and pasture (or “crop”): evergreen needleleaf forest (or “pine” as before), cropland/woodland mosaic (“crop/wood” as before), deciduous broadleaf forest (“deciduous”), and mixed forest (Figure 2). The region where pine is converted to crop, the largest LULCC

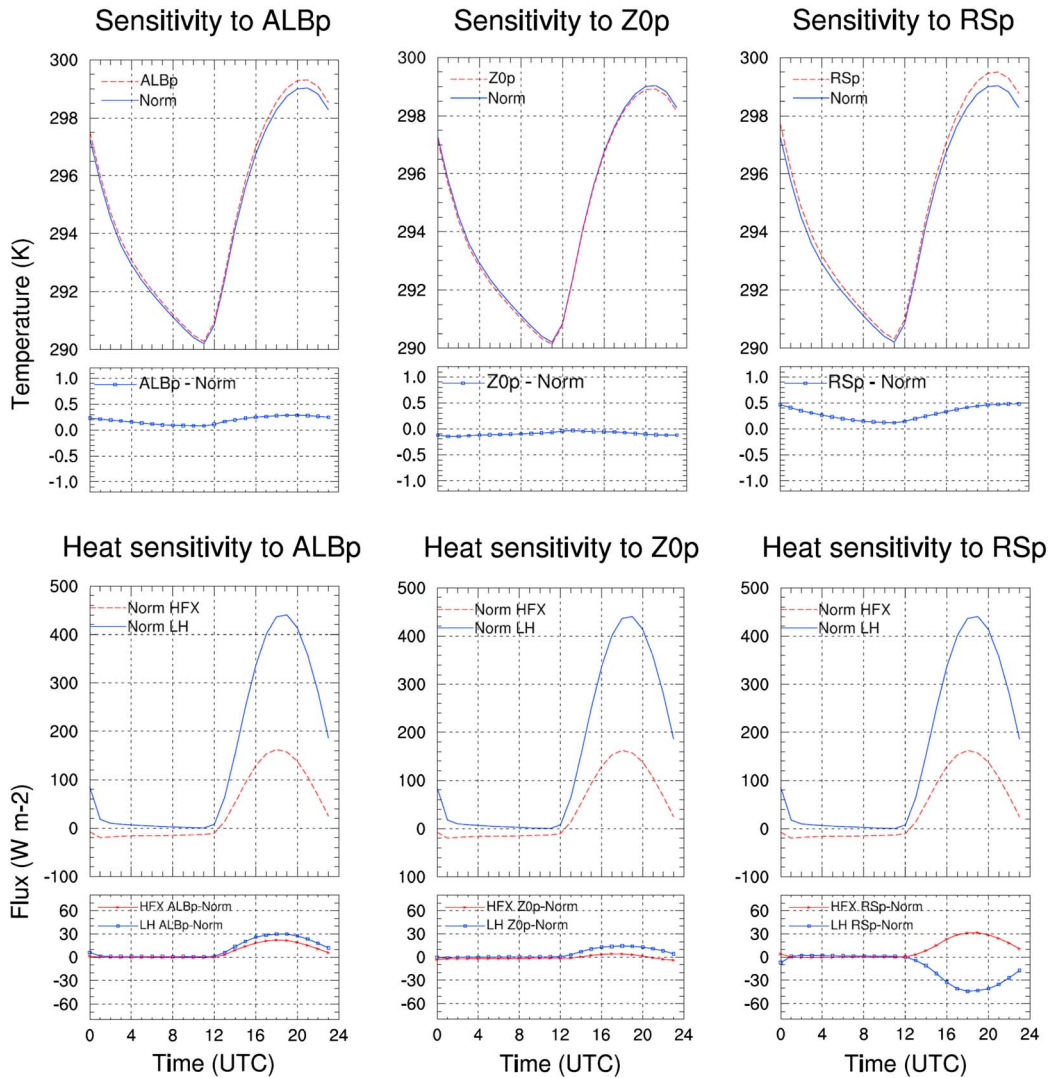


Figure 7. Average diurnal temperature and heat flux trends and sensitivities to (left column) pine albedo (ALBp), (middle column) surface roughness (Z^0p), and (right column) stomatal resistance (RSp) over the grid cells where the dominant land use is crop during summer of the year 2050. (top row) Average diurnal surface temperature of the base case (blue) and the perturbed parameter simulation (red). (second row) Average diurnal surface temperature sensitivity (perturbed case minus base case). (third row) Average diurnal sensible (red) and latent (blue) heat flux to the atmosphere for the base case. (bottom row) Average diurnal sensible (red) and latent (blue) heat flux sensitivities (perturbed case minus base case).

in this scenario, covers almost all of Louisiana, Mississippi, Alabama, Georgia, and South Carolina except where crop already existed. The pine to crop conversion also extends to southern Arkansas and northern Florida. In this scenario, crop/wood is converted to crop in the same regions where crop/wood is converted to pine in the Southeast reforestation scenario discussed earlier. Deciduous forest is converted to crop in large regions of northern Arkansas and southern Missouri, as well as some parts of Tennessee. Some mixed forest is converted to crop in eastern Tennessee and parts of North Carolina.

[22] In this scenario the albedo increases for all LULCC and all seasons except for regions where mixed forest is converted to crop (Figure S6a). The most dramatic increase of albedo is in the large regions where pine is converted, due to the year round low albedo of pine. Spring and summer see a less intense increase (around 5%) in albedo when the

crops emerge. Also, during the spring and summer, the albedo of crop/wood, deciduous, and mixed forest are all nearly the same as that of crop (0.16 to 0.17 from Table 2).

[23] The LAI decreases with the conversion of pine to crop mostly during the winter (up to 3.5 units area^{-1}), less during the spring and fall (around 2 units area^{-1}), and only slightly during the summer (less than 1 unit area^{-1}) (Figure S6b). The LAI also decreases slightly for all other LULCC during the winter. However, during the summer, the LAI increases for all other LULCC with the highest increase over regions where deciduous is converted to crop (more than 2 units area^{-1}). In this scenario, RS decreases from between 70 and 125 s m^{-1} to 40 s m^{-1} . The surface roughness decreases for all LULCC and for all seasons with the biggest decreases happening during the winter where pine and deciduous change to crop.

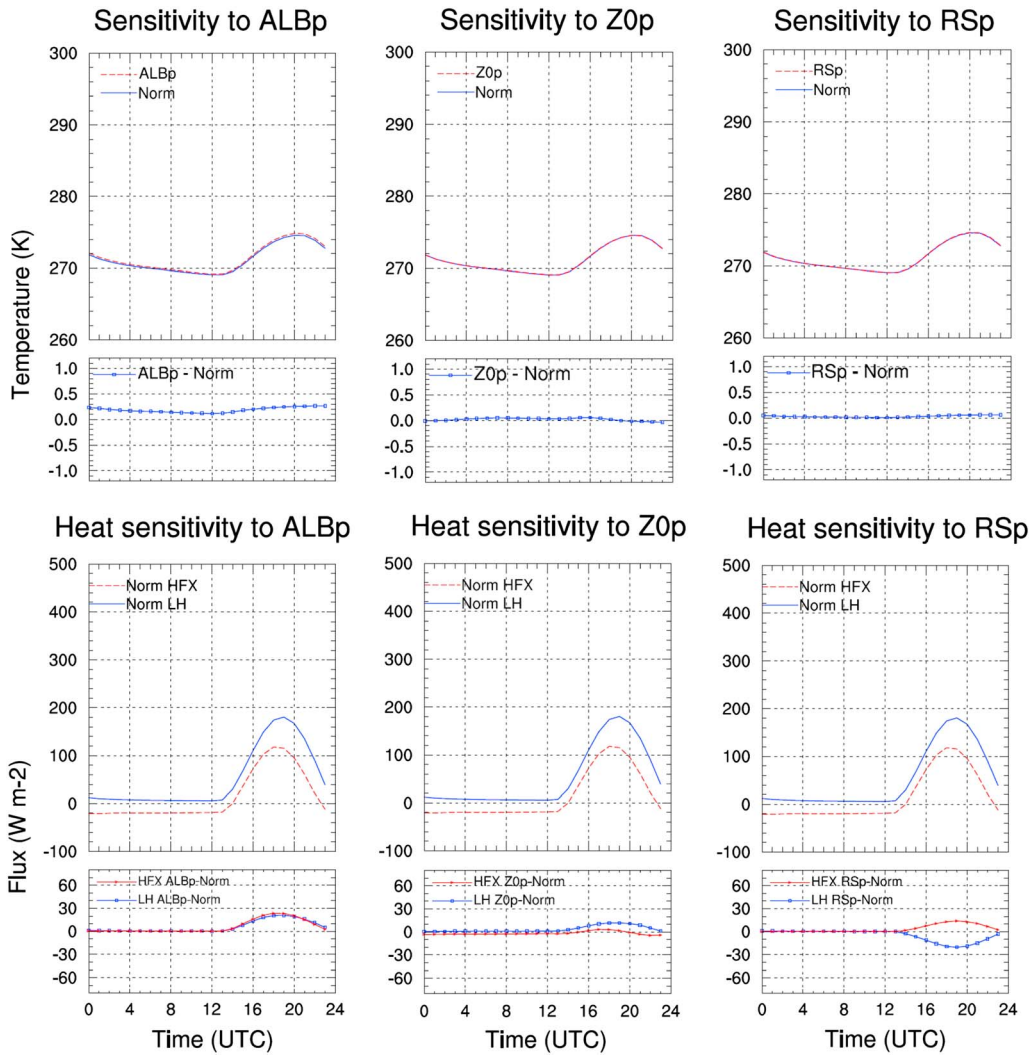


Figure 8. Average diurnal temperature and heat flux trends and sensitivities to (left column) pine albedo (ALBp), (middle column) surface roughness (Z^0_p), and (right column) stomatal resistance (RSp) over grid cells where the dominant land use is crop during winter of the year 2050. (top row) Average diurnal surface temperature of the base case (blue) and the perturbed parameter simulation (red). (second row) Average diurnal surface temperature sensitivity (perturbed case minus base case). (third row) Average diurnal sensible (red) and latent (blue) heat flux to the atmosphere for the base case. (bottom row) Average diurnal sensible (red) and latent (blue) heat flux sensitivities (perturbed case minus base case).

3.2.2. Impacts on Meteorology

[24] Most regions in the Southeast are cooled with future cropification (Figure 5a) with the largest and most significant (Figure A2; p values < 0.05) decreases occurring during the summer over northern Mississippi and Alabama and southern Tennessee (over 0.6° decrease). Similarly, decreases in surface air heat content are found over most of the region of LULCC (Figure 5c). During the winter, average cooling during the hottest hour of the day reaches 0.5° over regions where pine is converted to crop (Figure S7). Increases in albedo over regions where deciduous and pine forests are converted to crop drives the cooling during the winter, despite the warming effect that is expected from the decrease in Z^0 and latent heat flux. Also, boundary layer height during the daytime drops by an average of 100 m (more than 10% decrease) where pine changes to crop (Figure S7),

and slightly less where deciduous changes to crop, because boundary layer depth is reduced when less of the energy flux is realized as sensible heat [Pielke *et al.*, 1998].

[25] In the spring and summer, most of the cooling occurs over regions where deciduous is converted to crop (reaching up to 0.8° decrease in some areas), and less cooling is seen over other LULCC regions. Cooling in converted deciduous regions is driven by an increase in the albedo and decreased RS. Diurnal heat flux trends (Figure 6) show a decrease in sensible heat flux and an increase in latent heat flux, due to the combined effect of albedo change and increased evapotranspiration from combined RS and LAI change. In contrast, regions changed from pine experience less cooling, because LAI and Z^0 decreases exert a warming force via latent heat flux decreases (Figure 6). There is also less soil moisture available for evaporation due to a decrease in RS in some regions (Figure 5b).

3.3. Integration of Sensitivity Analysis

[26] Sensitivity analyses were conducted to test the sensitivity of regional climate to albedo, surface roughness, leaf area index, and stomatal resistance. The sensitivity analyses find that surface temperatures and energy flux distributions are more sensitive to RS during the summer than all other sensitivity scenarios (Figure 7) with average surface temperatures increasing by 0.5° during the daytime. Winter temperature and surface fluxes are not sensitive to RS since evaporation is minimal, as is the related energy flux when crops are not in season. Surface temperature and energy flux over cropland are less sensitive to increasing the cropland LAI as compared to those of pine; however, when the cropland LAI is reduced to that of deciduous forest, the temperature increases slightly during the summer (Figure S8). During summer and winter, the daytime surface temperature in grids dominated by cropland increases by 0.2° when crop albedo is replaced by that of pine. The sensible and latent heat fluxes also increase (Figures 7 and 8). During summer, temperatures tend to decrease due to an increased surface roughness by 0.1° , while the latent heat is increased and the sensible heat decreased (Figure 7). Temperature and energy fluxes are less sensitive to Z^0 during the winter (Figure 8). Sensitivity analyses were also conducted using North American Regional Reanalysis (NARR) data as initial and boundary conditions. These sensitivity analyses were conducted with and without using spectral nudging and using 2010 NARR data (Figures S9 through S12). In the case where spectral nudging is used (Figures S9 and S10), the sensitivity results are nearly identical to the results using GISS fields as initial and boundary conditions. With no spectral nudging (Figures S11 and S12), we see increased sensitivity of surface temperature to albedo and stomatal resistance, while the sensitivity to surface roughness and leaf area index remain near zero.

4. Discussion

[27] The simulated impacts of LULCC in the Southeast on regional climate were expected given the changes in land use parameters (e.g., albedo, RS, LAI, and Z^0). Reforestation of crop regions in the Southeast tends to lead to warming primarily due to the increase of RS and decrease in albedo, while the Z^0 increase may lessen the degree of warming by shifting the transfer of energy to the atmosphere from sensible to latent heat. Warming during the spring, summer, and fall can enhance the production of O_3 and secondary particulate matter (PM) while, on the other hand, the increased boundary layer height can help decrease concentrations. Warming during the winter may influence less use of wood burning stoves and therefore lead to less emission of PM [Alfarra et al., 2007]. This result compares well with other studies on the impacts of reforestation on climate [Beltran-Przekurat et al., 2012; Betts, 2000; Betts et al., 2007]. However, over time, reduced transpiration from increased RS can lead to the accumulation of soil moisture in wet areas such that cooling from soil moisture evaporation overcomes the warming from albedo changes, which is the case for the afforested summer and fall in Louisiana near the Mississippi river. Lawrence and Chase [2010] found similar cooling from reforestation.

[28] Our results suggest that cooling tends to occur when forest is replaced with crop in the Southeast, though not

enough to counter the simulated warming of $1\text{--}3^{\circ}\text{C}$ from greenhouse gas increases [Trail et al., 2013]. Cooling during the winter is attributed to the high albedo of cropland, while during the spring and summer, the decrease in RS also contributes to cooling. Also, increased LAI helps cool where deciduous forests are replaced. These results agree with other studies simulating the impacts of cropification [Beltran-Przekurat et al., 2012; Davin and de Noblet-Ducoudre, 2010] as well as looking at historical LULCC and temperature data [Fall et al., 2010b]. Cooling during the winter could cause more emissions of PM from wood burning, while during the rest of the year, the rate of production of O_3 and secondary PM could decrease.

[29] While the results of the LULCC study show that reforestation of cropland does not appear to be an effective method for climate mitigation in the Southeast, the sensitivity analysis shows that these results are sensitive to assumed physical parameters. Some recent studies have found a significant degree of cooling from reforestation in the Southeast [Juang et al., 2007; Murphy et al., 2012]. In particular, Murphy et al. suggest that the stomatal conductance of loblolly pine, the major species of pine in the Southeast, should be adjusted from the default value and this would lead to more simulated cooling in the Southeast [Murphy et al., 2012]. We assumed the default value for stomatal resistance from the USGS 24-category land use data for a combined “evergreen needleleaf” category. Thus, further investigation is needed to minimize uncertainty in the stomatal resistance and to consider the physiological differences between actual loblolly pine and the evergreen needleleaf category typically used, as well as the physiological differences among the various crops present in the Southeast. Our results suggest that a reduction in the stomatal resistance of pine equivalent to the Murphy simulations would lead to a cooler surface over pine forest. Juang et al. found that in a region of North Carolina, pine forest tend to be cooler than marginal, or abandoned, fields [Juang et al., 2007]. These fields have less leaf area and lower roughness heights than cropland and are not subject to irrigation, all of which would tend to make marginal fields warmer than cropland and potentially warmer than pine forest, especially loblolly pine.

[30] **Acknowledgments.** While this work was supported, in part, by grants from the US EPA (EPA-G2008-STAR-J1) and NASA, reference herein to any specific commercial products, process, or service by trade name, trademark, manufacturer, or otherwise, does not necessarily constitute or imply their endorsement or recommendation. NARR data were provided by the NOAA/OAR/ESRL PSD, Boulder, Colorado, USA, from their Web site at <http://www.esrl.noaa.gov/psd/>. The views and opinions expressed herein are those of the authors and do not necessarily state or reflect those of the United States Government.

References

- Akhtar, F., M. E. Chang, and A. G. Russell (2008), Beyond the standards: Designer air quality in 2050, *Bull. Am. Meteorol. Soc.*, *89*(1), 38–38.
- Alfarra, M. R., et al. (2007), Identification of the mass spectral signature of organic aerosols from wood burning emissions, *Environ. Sci. Technol.*, *41*(16), 5770–5777, doi:10.1021/es062289b.
- Arora, V. K., and A. Montenegro (2011), Small temperature benefits provided by realistic afforestation efforts, *Nat. Geosci.*, *4*(8), 514–518, doi:10.1038/ngeo1182.
- Bala, G., K. Caldeira, A. Mirin, M. Wickett, and C. Delire (2005), Multicentury changes to the global climate and carbon cycle: Results from a coupled climate and carbon cycle model, *J. Clim.*, *18*(21), 4531–4544, doi:10.1175/jcli3542.1.
- Bala, G., K. Caldeira, M. Wickett, T. J. Phillips, D. B. Lobell, C. Delire, and A. Mirin (2007), Combined climate and carbon-cycle effects of large-scale

- deforestation, *Proc. Natl. Acad. Sci. U. S. A.*, 104(16), 6550–6555, doi:10.1073/pnas.0608998104.
- Beltran-Przekurat, A., R. A. Pielke Sr., J. L. Eastman, and M. B. Coughenour (2012), Modelling the effects of land-use/land-cover changes on the near-surface atmosphere in southern South America, *Int. J. Climatol.*, 32(8), 1206–1225, doi:10.1002/joc.2346.
- Betts, R. A. (2000), Offset of the potential carbon sink from boreal forestation by decreases in surface albedo, *Nature*, 408(6809), 187–190, doi:10.1038/35041545.
- Betts, R. A., P. D. Falloon, K. K. Goldewijk, and N. Ramankutty (2007), Biogeophysical effects of land use on climate: Model simulations of radiative forcing and large-scale temperature change, *Agric. For. Meteorol.*, 142(2–4), 216–233, doi:10.1016/j.agrformet.2006.08.021.
- Bull, S. R. (1996), Renewable energy transportation technologies, *Renewable Energy*, 9(1–4), 1019–1024.
- Cai, M., and E. Kalnay (2004), Climate: Impact of land-use change on climate—Reply, *Nature*, 427(6971), 214–214, doi:10.1038/427214a.
- Castro, C. L., R. A. Pielke Sr., and Giovanni Leoncini (2005), Dynamical downscaling: Assessment of value retained and added using the regional atmospheric modeling system (RAMS), *J. Geophys. Res.*, 110, D05108, doi:10.1029/2004JD004721.
- Chase, T. N., R. A. Pielke Sr., T. G. F. Kittel, R. R. Nemani, and S. W. Running (2000), Simulated impacts of historical land cover changes on global climate in northern winter, *Clim. Dyn.*, 16(2–3), 93–105, doi:10.1007/s003820050007.
- Chen, H., H. Tian, M. Liu, J. Melillo, S. Pan, and C. Zhang (2006), Effect of land-cover change on terrestrial carbon dynamics in the southern United States, *J. Environ. Qual.*, 35(4), 1533–1547, doi:10.2134/jeq2005.0198.
- Christy, J. R., W. B. Norris, K. Redmond, and K. P. Gallo (2006), Methodology and results of calculating central California surface temperature trends: Evidence of human-induced climate change?, *J. Clim.*, 19(4), 548–563, doi:10.1175/jcli3627.1.
- Conner, R. C., and A. J. Hartsell (2002), *The Southern Forest Resource Assessment: Chapter 16, Forest Area and Conditions*, Department of Agriculture, Forest Service, Southern Research Station, Asheville, NC.
- Davin, E. L., and N. de Noblet-Ducoudre (2010), Climatic impact of global-scale deforestation: Radiative versus nonradiative processes, *J. Clim.*, 23(1), 97–112, doi:10.1175/2009jcli3102.1.
- Dudhia, J. (1989), Numerical study of convection observed during the winter monsoon experiment using a mesoscale two-dimensional model, *J. Atmos. Sci.*, 46(20), 3077–3107.
- Ek, M. B., et al. (2003), Implementation of Noah land surface model advances in the National Centers for Environmental Prediction operational mesoscale Eta model, *J. Geophys. Res.*, 108(D22), 8851, doi:10.1029/2002JD003296.
- Fall, S., N. S. Diffenbaugh, D. Niyogi, R. A. Pielke Sr., and G. Rochon (2010a), Temperature and equivalent temperature over the United States (1979–2005), *Int. J. Climatol.*, 30(13), 2045–2054, doi:10.1002/joc.2094.
- Fall, S., D. Niyogi, A. Gluhovsky, R. A. Pielke Sr., E. Kalnay, and G. Rochon (2010b), Impacts of land use land cover on temperature trends over the continental United States: Assessment using the North American Regional Reanalysis, *Int. J. Climatol.*, 30(13), 1980–1993, doi:10.1002/joc.1996.
- Hong, S. Y., Y. Noh, and J. Dudhia (2006), A new vertical diffusion package with an explicit treatment of entrainment processes, *Mon. Weather Rev.*, 134(9), 2318–2341.
- IPCC (Intergovernmental Panel on Climate Change) (2007), Climate change 2007 IPCC fourth assessment report: Synthesis report, 184 pp, IPCC, Geneva, Switzerland.
- Juang, J. Y., G. Katul, M. Siqueira, P. Stoy, and K. Novick (2007), Separating the effects of albedo from eco-physiological changes on surface temperature along a successional chronosequence in the southeastern United States, *Geophys. Res. Lett.*, 34, L21408, doi:10.1029/2007GL031296.
- Kain, J. S., and J. M. Fritsch (1993), Convective parameterization models: The Kain–Fritsch scheme. Cumulus convection in numerical models, *Am. Meteorol. Soc.*, 46, 165–170.
- Kalnay, E., and M. Cai (2003), Impact of urbanization and land-use change on climate, *Nature*, 423(6939), 528–531, doi:10.1038/nature01675.
- Lamarque, J. F., G. P. Kyle, M. Meinshausen, K. Riahi, S. J. Smith, D. P. van Vuuren, A. J. Conley, and F. Vitt (2011), Global and regional evolution of short-lived radiatively-active gases and aerosols in the Representative Concentration Pathways, *Clim. Change*, 109(1–2), 191–212, doi:10.1007/s10584-011-0155-0.
- Lawrence, P. J., and T. N. Chase (2007), Representing a new MODIS consistent land surface in the Community Land Model (CLM 3.0), *J. Geophys. Res.*, 112, G01023, doi:10.1029/2006JG000168.
- Lawrence, P. J., and T. N. Chase (2010), Investigating the climate impacts of global land cover change in the community climate system model, *Int. J. Climatol.*, 30(13), 2066–2087, doi:10.1002/joc.2061.
- Leiby, P. N., and J. Rubin (2003), Transitions in light-duty vehicle transportation: Alternative-fuel and hybrid vehicles and learning, in *Energy, Air Quality, and Fuels 2003*, edited, pp. 127–134.
- Lin, Y. L., et al. (1983), Bulk parameterization of the snow field in a cloud model, *J. Climate Appl. Meteorol.*, 22(6), 1065–1092, doi:10.1175/1520-0450(1983)022.
- Liu, P., A. P. Tsimpidi, Y. Hu, B. Stone, A. G. Russell, and A. Nenes (2012), Differences between downscaling with spectral and grid nudging using WRF, *Atmos. Chem. Phys.*, 12(8), 3601–3610, doi:10.5194/acp-12-3601-2012.
- Mahmood, R., et al. (2010), Impacts of land use/land cover change on climate and future research priorities, *Bull. Am. Meteorol. Soc.*, 91, 37–46, doi:10.1175/2009bams2769.1.
- Marti, O., et al. (2005), The new IPSL climate system model: IPSL-CM4, *Note du Pole de Modelisation*, 26, 86.
- Mlawer, E. J., et al. (1997), Radiative transfer for inhomogeneous atmospheres: RRTM, a validated correlated-k model for the longwave, *J. Geophys. Res.*, 102(D14), 16,663–16,682, doi:10.1029/97JD00237.
- Moss, R. H., et al. (2010), The next generation of scenarios for climate change research and assessment, *Nature*, 463(7282), 747–756, doi:10.1038/nature08823.
- Murphy, L. N., W. J. Riley, and W. D. Collins (2012), Local and remote climate impacts from expansion of woody biomass for bioenergy feedstock in the southeastern United States, *J. Clim.*, 25(21), 7643–7659, doi:10.1175/jcli-d-11-00535.1.
- NRC (2005), Radiative forcing of climate change: Expanding the concept and addressing uncertainties, *National Research Council*, 208.
- Nunez, M. N., et al. (2008), Impact of land use and precipitation changes on surface temperature trends in Argentina, *J. Geophys. Res.*, 113, D06111, doi:10.1029/2007JD008638.
- Pacala, S. W., et al. (2001), Consistent land- and atmosphere-based US carbon sink estimates, *Science*, 292(5525), 2316–2320, doi:10.1126/science.1057320.
- Pielke, R. A., R. Avissar, M. Raupach, A. J. Dolman, X. B. Zeng, and A. S. Denning (1998), Interactions between the atmosphere and terrestrial ecosystems: Influence on weather and climate, *Glob. Change Biol.*, 4(5), 461–475, doi:10.1046/j.1365-2486.1998.101-1-00176.x.
- Pielke, R. A., et al. (2011), Land use/land cover changes and climate: Modeling analysis and observational evidence, *Wiley Interdiscip. Rev.-Clim. Chang.*, 2(6), 828–850, doi:10.1002/wcc.144.
- Prestemon, J. P., and R. C. Abt (2002), The Southern timber market to 2040, *J. For.*, 100(7), 16–22.
- Skamarock, W. C., and J. B. Klemp (2008), A time-split nonhydrostatic atmospheric model for weather research and forecasting applications, *J. Comput. Phys.*, 227(7), 3465–3485, doi:10.1016/j.jcp.2007.01.037.
- Skamarock, W., J. B. Klemp, J. Dudhia, D. O. Gill, D. Barker, M. G. Duda, X.-Y. Huang, and W. Wang (2005), A description of the advanced research WRF version 2.
- Song, J., A. Webb, B. Parmenter, D. T. Allen, and E. McDonald-Buller (2008), The impacts of urbanization on emissions and air quality: Comparison of four visions of Austin, Texas, *Environ. Sci. Technol.*, 42(19), 7294–7300.
- Stauffer, D. R., and N. L. Seaman (1990), Use of four-dimensional data assimilation in a limited-area mesoscale model. 1. Experiments with synoptic-scale data, *Mon. Weather Rev.*, 118(6), 1250–1277, doi:10.1175/1520-0493(1990)118.
- Steyaert, L. T., and R. G. Knox (2008), Reconstructed historical land cover and biophysical parameters for studies of land-atmosphere interactions within the eastern United States, *J. Geophys. Res.*, 113, D02101, doi:10.1029/2006JD008277.
- Stooksbury, D. (2008), A primer on drought history in Georgia, in *Georgia Climate and Air Quality Summit*, edited, Atlanta, GA.
- Thompson, S. L., et al. (2004), Quantifying the effects of CO₂-fertilized vegetation on future global climate and carbon dynamics, *Geophys. Res. Lett.*, 31, L23211, doi:10.1029/2004GL021239.
- Trail, M., A. P. Tsimpidi, P. Liu, K. Tsigaridis, Y. Hu, A. Nenes, and A. G. Russell (2013), Downscaling a global climate model to simulate climate change impacts on US regional and urban air quality, *Geosci. Model Dev. Discuss.*, 6, 2517–2549, doi:10.5194/gmdd-6-2517-2013.
- Wear, D. N., and J. G. Greis (2002), Southern forest resource assessment - Summary of findings, *J. For.*, 100(7), 6–14.